

Warped Discrete S-Transform

Alam Silva Menezes and Moisés Vidal Ribeiro

Abstract—This work introduces the warped discrete-time S-transform and the warped discrete S-transform to improve the time frequency representation of the well-known S-transform. The proposed transforms make use of a non-uniform mapping of tones in the frequency domain to increase the time frequency resolution in a specified frequency band. Numerical results show that the warped discrete S-transform can offer better time-frequency representation than discrete S-transform and short time discrete Fourier transform. As a result, it has the potential to increase the performance of techniques based on S-transform that have been designed to analyze non-stationary signals. Finally, it is demonstrated that the discrete S-transform is a particular case of the warped discrete S-transform.

Keywords—Warped, S transform, Time-frequency representation, Warped S Transform.

I. INTRODUCTION

Time-frequency representation (TFR) techniques [1] are used to analyze non-stationary signals in electric power systems [2]. The classical TFR technique is the short-time Fourier transform (STFT). Basically, the STFT consists of applying a short time window on the signal in time and mapping it in the frequency domain using the Fourier transform. The drawbacks related to the STFT is a poor time resolution for frequency components localized in high frequency and frequency resolution with a severe limitation (e.g., it is $2\pi/N$, if its discrete version is applied to a N -length signal). On the other hand, the TFR technique called S -transform was proposed to solve the problem of low time resolution for components localized in high frequency [3]. Due to this characteristic, the S-transform has been extensively applied to analyze non-stationary signals, such as electric ones [2], [4] and [5]. However, the S-transform does not offer high TFR for components localized in high frequencies [6].

In this contribution, by introducing the warped discrete time S-transform (WDTST) and the warped discrete S-transform (WDST) this limitation of S-transform is overcome. The WDTST and WDST were first introduced in [7]. A warped S-transform was applied in [8] to analyse brain waves. However, [7] employs a first order all pass filter, on the other hand [8] uses a second order all pass filter in order to obtain the warped S-transform. The WDST is a discrete version of the WDTST and because of that it can be evaluated demanding computational complexity similar to the discrete S-transform (DST). The idea behind both WDTST and WDST techniques is the concept of warping frequency [9]-[10], in which the tones are non-uniformly mapped into the normalized spectrum.

Alam Silva Menezes, Service and Engineering Department, Petrobras Transporte SA, Rio de Janeiro, Brazil, E-mail: alamsm@petrobras.com.br. Moisés Vidal Ribeiro, Department of Electrical Engineering, Federal University of Juiz de Fora, Juiz de Fora-MG, Brazil, E-mail: mribeiro@engenharia.ufjf.br. This work was partially supported by INERGE and Transpetro.

As a result, an improved TFR can be achieved for *a priori* chosen frequency band. Then, the proposed warped S -transforms are capable of offering better TFR representations than the well-known DST and discrete STFT (STDFT). Numerical results based on non-stationary signals show this improvement. Finally, but not the least, we demonstrate that the DST is a particular case of the WDST.

This paper is organized as follow. In section II we review the concept of warped transform. Section III presents the discrete-time S transform (DTST). In section we introduce the transforms warped discrete-time transforms (WDTST) and warped discrete S transform (WDST). In section V we assess the techniques using two specific non-stationary signals. Finally, in section VI, we presents the conclusions and outline future works.

II. THE WARPED DISCRETE FOURIER TRANSFORM

The z -transform of $\{x[n]\}_{n=0}^{N-1}$ is defined by

$$X(z) \triangleq \sum_{n=0}^{N-1} x[n] z^{-n}, \quad (1)$$

the discrete Fourier transform (DFT) of $\{x[n]\}_{n=0}^{N-1}$ is defined by

$$X_{DFT}[k] \triangleq \frac{1}{N} \sum_{n=0}^{N-1} x[n] e^{-i\frac{2\pi}{N}kn}. \quad (2)$$

Considering the variable $z \triangleq e^{i\omega_k}$, where $\omega_k = 2\pi k/N$, we can see that the DFT is a sequence which is obtained by uniformly sampling the z -transform over unitary cycle in the z -plane, as shown in (3)

$$\begin{aligned} X[k] &= X(z)|_{z=e^{i2\pi k/N}} \\ &= \sum_{n=0}^{N-1} x[n] e^{-i(2\pi/N)kn}, \end{aligned} \quad (3)$$

with $0 \leq n \leq N-1$.

The discrete frequencies of the DFT ($\omega_k \triangleq 2\pi k/N$) are distributed in a regular fashion over unitary circle, as shown in Fig. 1. Note that the frequency resolution of DFT is given by $2\pi/N$. Therefore, the frequency resolution of DFT is constant for a given number of samples N and also uniform inside the interval $0 \leq \omega_k < 2\pi$. In an effort to increase the frequency resolution of DFT, it should be use a large number of frequency samples N .

The most simple approach applied to improve frequency resolution is the use of zero-padding, which increase the computational complexity. On the other hand, [9] shows that it is possible increase the frequency resolution at a specific region of unitary circle using the same numbers of discrete frequencies, N . To this end, [10] proposes replace the z

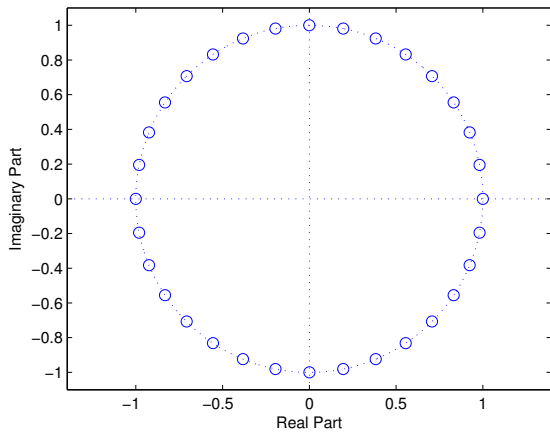
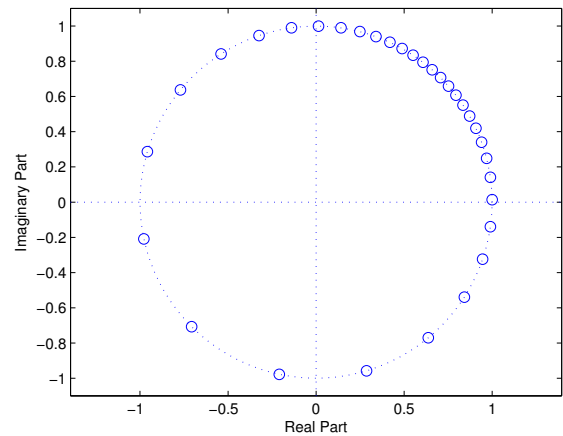


Fig. 1. Discrete frequencies of DFT over unitary circle.


 Fig. 2. WDFT with $a = 0,5e^{i\pi/4}$.

variable at z -transform (1) by a specific all pass filter, $B(z)$ as follow:

$$\overline{X}(z) \triangleq \sum_{n=0}^{N-1} x[n] B(z)^n. \quad (4)$$

Where we assume that $B(z)$ is a 1st-order all pass filter such that

$$B(z) = \frac{a^* + z^{-1}}{1 + az^{-1}}, \quad (5)$$

in which $a = \alpha e^{i\varphi} \in \mathbb{C}$.

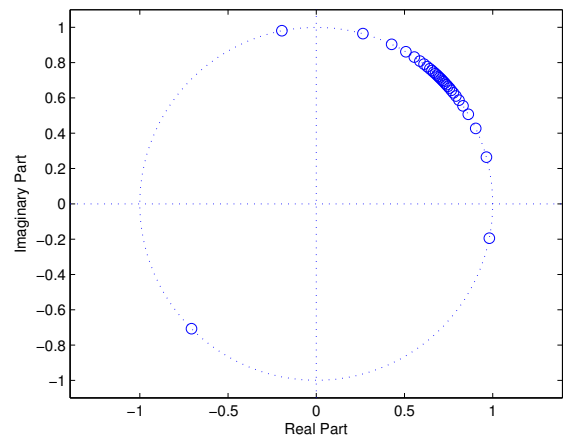
In this way, considering $z = e^{i\omega_k}$ ($\omega_k \in [0, 2\pi)$), [10] proposes the warped discrete Fourier transform (WDFT), which is defined by

$$X[\varpi_k] \triangleq \frac{1}{N} \sum_{n=0}^{N-1} x[n] \left(\frac{a^* + e^{i\omega_k}}{1 + ae^{i\omega_k}} \right)^n, \quad (6)$$

where $\omega_k \triangleq \arg\{e^{i\omega_k}\}$ is the k th discrete frequency and $\varpi_k \triangleq \arg\{B(z)|_{z=e^{i\omega_k}}\}$ refers to the k th warped discrete frequency.

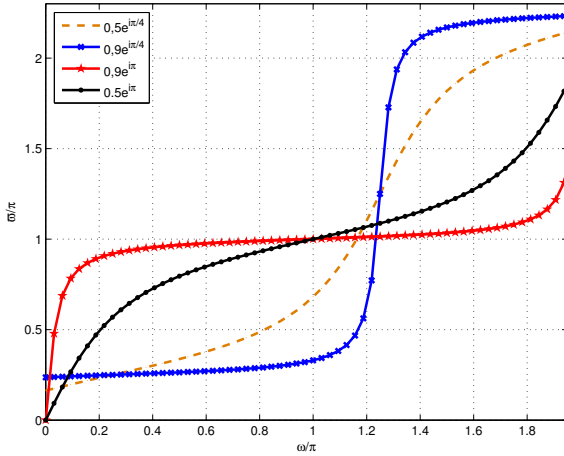
Note that the DFT is a special case of WDFT when $a = 0$. The effect of parameter $a = \alpha e^{i\varphi}$ at discrete frequencies of the WDFT is shown in Figs. 2 and 3. As we can see, φ is the frequency over unitary circle where the discrete frequencies are placed. On the other hand, the parameter α defines the concentration of frequencies around φ .

The relationship between ϖ_k and ω_k is given by


 Fig. 3. WDFT with $a = 0,9e^{i\pi/4}$.

$$\begin{aligned} \varpi &= \arg \left\{ \frac{1+az^{-1}}{a^*+z^{-1}} \right\} \\ &= \arg \left\{ \frac{1+ae^{-i\omega}}{a^*+e^{-i\omega}} \right\} \\ &= \arg \left\{ \frac{1+ae^{-i\omega}}{e^{-i\omega}(1+a^*e^{i\omega})} \right\} \\ &= \arg \{e^{i\omega}\} + \arg \left\{ \frac{1+ae^{-i\omega}}{(1+a^*e^{i\omega})} \right\} \\ &= \omega + \arg \left\{ \frac{(1+ae^{-i\omega})(1+ae^{-i\omega})}{(1+a^*e^{i\omega})(1+ae^{-i\omega})} \right\} \\ &= \omega + \arg \left\{ \left(\frac{1+ae^{-i\omega}}{1+a^*e^{i\omega}} \right)^2 \right\} \\ &= \omega + 2 \arg \left\{ (1 + \alpha e^{i\varphi} e^{-i\omega}) \right\} \\ &= \omega + 2 \arg \left\{ 1 + \cos(\varphi - \omega) + j \sin(\varphi - \omega) \right\} \\ &= \omega + 2 \tan^{-1} \left(\frac{\alpha \sin(\varphi - \omega)}{1 + \alpha \cos(\varphi - \omega)} \right), \end{aligned} \quad (7)$$

because $\omega_k \triangleq \arg\{e^{i\omega_k}\}$ and $\varpi_k \triangleq \arg\{B(z)|_{z=e^{i\omega_k}}\}$. Fig. 4 shows graphically the effect of parameter a in the relationship between ϖ_k and ω_k .


 Fig. 4. Mapping between frequencies ω and ϖ .

III. DISCRETE-TIME S TRANSFORM

The S-transform of a signal $x(t) \in \mathbb{R} \mid \forall t \in \mathbb{R}$ is given by

$$\begin{aligned} S(\tau, f) &= \int_{-\infty}^{\infty} x(t) g(\tau - t, f) e^{-i2\pi ft} dt \\ &= \int_{-\infty}^{\infty} x(t) \frac{|f|}{\sqrt{2\pi}} e^{-\frac{1}{2}[(\tau-t)^2 f^2]} e^{-i2\pi ft} dt, \end{aligned} \quad (8)$$

in which $\tau \in \mathbb{R}$ and $f \in \mathbb{R}$ denote time instant in second (s) and frequency in Hertz (Hz), respectively. Also, it is assumed that

$$g(t, f) = \frac{|f|}{\sqrt{2\pi}} e^{-(t^2/2\sigma^2)} \quad (9)$$

with $\sigma = 1/|f|$ is a Gaussian function.

Let $\{x[n]\}_{n=0}^{N-1}$ such that $x[n] = x(t)|_{t=nT_s}$, where $T_s = 1/2B$ with $B \in \mathbb{R}$ and $X(j\Omega) = 0, \forall |\Omega| \geq 1/2B$ in which $X(j\Omega)$ is the Fourier transform of $x(t)$. Then, the DST of $\{x[n]\}_{n=0}^{N-1}$ can be expressed by

$$S[d, k] = \frac{1}{\sqrt{2\pi}} \sum_{n=0}^{N-1} x[n] \frac{k}{N} e^{-\frac{1}{2}[(d-n)\frac{k}{N}]^2} e^{-i\frac{2\pi}{N}kn}, \quad (10)$$

where $d, k \in \mathbb{Z}$ refer to the discretization of τ and f . Note that $d, k, n \in \gamma = \{0, 1, \dots, N-1\}$.

IV. THE WARPED DISCRETE S TRANSFORM

Let rewrite the DST as follows:

$$S[d, k] = \frac{1}{\sqrt{2\pi}} \sum_{n=0}^{N-1} x[n] \frac{2\pi k}{2\pi N} e^{-\frac{1}{2}[(d-n)\frac{2\pi k}{2\pi N}]^2} e^{-i\frac{2\pi}{N}kn}. \quad (11)$$

Now, we assume that $z = e^{i\frac{2\pi}{N}k}$ and $\arg\{z\} = \frac{2\pi}{N}k$ because we are over the unitary circle, then

$$\begin{aligned} S\left[d, \frac{N}{2\pi} \arg\{z\}\right] &= \\ \frac{1}{\sqrt{2\pi}} \sum_{n=0}^{N-1} x[n] \frac{\arg\{z\}}{2\pi} e^{-\frac{1}{2}[(d-n)\frac{\arg\{z\}}{2\pi}]^2} z^{-n}. \end{aligned} \quad (12)$$

If we replace z^{-1} by the all pass filter $B(z)$, equation (5), we have

$$\begin{aligned} S\left[d, \frac{N}{2\pi} \arg\{B(z)\}\right] &= \\ \frac{1}{\sqrt{2\pi}} \sum_{n=0}^{N-1} x[n] \frac{\arg\{B(z)\}}{2\pi} e^{-\frac{1}{2}[(d-n)\frac{\arg\{B(z)\}}{2\pi}]^2} B(z)^n. \end{aligned} \quad (13)$$

From which we defined the WDTST as follow

$$S\left[d, \frac{N}{2\pi} \varpi\right] \triangleq \frac{1}{\sqrt{2\pi}} \sum_{n=0}^{N-1} x[n] \frac{\varpi}{2\pi} e^{-\frac{1}{2}[(d-n)\frac{\varpi}{2\pi}]^2} B(e^{i\omega})^n, \quad (14)$$

where

$$\begin{aligned} \varpi &= \arg\{B(e^{i\omega})\} \\ &= \omega + 2 \arctan(\beta) \end{aligned} \quad (15)$$

with $0 \leq \omega < 2\pi$ and $\beta = \frac{|a| \sin(\varphi - \omega)}{1 + |a| \cos(\varphi - \omega)}$. Note that a is a so-called warping parameter.

By applying (15) in (14) we obtain

$$\begin{aligned} S\left[d, \frac{N}{2\pi} [\omega + 2 \arctan(\beta)]\right] &= \frac{1}{2\pi\sqrt{2\pi}} \sum_{n=0}^{N-1} x[n] \times \\ &[\omega + 2 \arctan(\beta)] e^{-\frac{1}{2}[(d-n)\frac{\omega + 2 \arctan(\beta)}{2\pi}]^2} B(e^{i\omega})^n. \end{aligned} \quad (16)$$

As the computational complexity of WDTST is huge ($\omega \in [0, 2\pi)$), we define its discrete version as follows:

Let the uniform discretization of $\omega \in [0, 2\pi)$ result in $\omega_k = \frac{2\pi}{N}k$, then the WDST is define as

$$\begin{aligned} S\left[d, k + \frac{N}{\pi} \arctan(\beta_d)\right] &\triangleq \frac{1}{\sqrt{2\pi N}} \sum_{n=0}^{N-1} x[n] \times \\ &\left[k + \frac{N}{\pi} \arctan(\beta_d)\right] e^{-\frac{1}{2}[(d-n)(k + \frac{N}{\pi} \arctan(\beta_d))]^2} B\left(e^{i\frac{2\pi}{N}k}\right)^n \end{aligned} \quad (17)$$

in which $\beta_d = \frac{|a| \sin(\varphi - \frac{2\pi}{N}k)}{1 + |a| \cos(\varphi - \frac{2\pi}{N}k)}$.

For the sake of clarity, we can express (17) as the sum of two terms:

$$\begin{aligned} S\left[d, k + \frac{N}{\pi} \arctan(\beta_d)\right] &= \frac{1}{\sqrt{2\pi N}} \left\{ \right. \\ &\sum_{n=0}^{N-1} x[n] k e^{-\frac{1}{2}[(d-n)(k + \frac{N}{\pi} \arctan(\beta_d))]^2} B\left(e^{i\frac{2\pi}{N}k}\right)^n + \\ &\sum_{n=0}^{N-1} x[n] \left(\frac{N}{\pi} \arctan(\beta_d)\right) e^{-\frac{1}{2}[(d-n)(k + \frac{N}{\pi} \arctan(\beta_d))]^2} \times \\ &\left. B\left(e^{i\frac{2\pi}{N}k}\right)^n \right\} \end{aligned} \quad (18)$$

Note that if $a = 0$, then $S\left[d, k + \frac{N}{\pi} \arctan(\beta_d)\right] = S[d, k]$. It means that DST is a particular case of the WDST. Similar to the warped discrete Fourier Transform, the parameters $\alpha \in \mathbb{R} \mid 0 \leq \alpha < 1$ and $\varphi \in \mathcal{J} \mid \mathcal{J} = \left\{0, \frac{2\pi}{N}, \frac{4\pi}{N}, \dots, \frac{2\pi(N-1)}{N}\right\}$ control the concentration of tones in a portion of the normalized spectrum and

determines the tone around the concentration take place, respectively. Due this feature, the WDST can offer high resolution in both low and high frequencies. By offering high resolution in high frequency, the WDST overcomes the limitation of the DST reported in [3].

V. SIMULATIONS RESULTS

A comparative analysis among the WDST, the DST, and the STDFT is carried out by considering a non-stationary signal described in [3], which is reproduced in Fig. 5. This N -length and discrete-time signal is composed of two sinusoidal components whose frequencies in radians per sample are $(50/128)\pi$ and $(12/128)\pi$, respectively. Also, a short time duration sinusoidal component with a frequency equal to $(104/128)\pi$ is added.

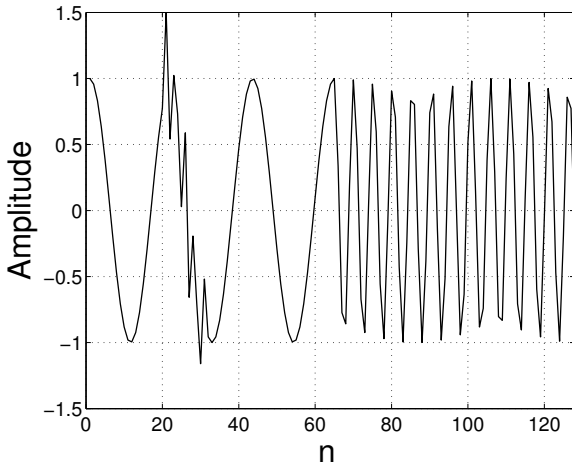


Fig. 5. Non-stationary signal in time domain.

The spectrograms obtained by using these TFR techniques are depicted in Figs. 6, 7 and 8, respectively. As it is well known in literature, the STDFT offers a poor time resolution for high frequency content. In Fig. 3 we see that the DST can achieve a better TFR than the STDFT (Fig. 2), which is also presented in literature. The spectrogram obtained with WDST is shown in Fig. 4. For this plot, we assume that $a = 0.7e^{i0.4\pi}$. One can see that the time resolution for high frequency content is maintained, see the detection of the short time duration signal. Due to concentration of tones around $\omega = 0.4\pi$ ($\varphi = 0.4\pi$), the signal whose frequency is $(50/128)\pi$ is better characterized by using WDST than the DST.

A phase voltage signal with harmonic distortion is also used to compare the WDST, the DST, and the STDFT, as shown in Fig. 9. The spectrogram generated by the STDFT (Fig. 10) is not able to show clearly the harmonic components and the high frequency distortion present in the voltage waveform. However, the DST can achieve a better TRF than STDFT as could be seen in Fig. 11. In fact, the harmonic components is evident at spectrogram around $\omega = 0.04$ (rad/sample). But, the high frequency component around sample $n = 200$ is spreaded over a great portion of normalized spectrum. It occurs because the DST offers a poor frequency-resolution for high frequency

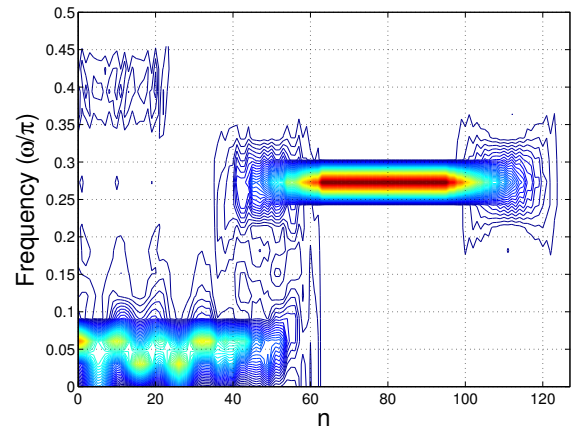


Fig. 6. The spectrogram provided by the STDFT.

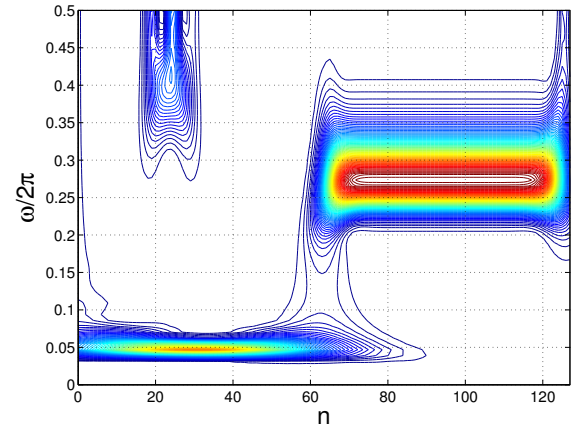


Fig. 7. The spectrogram provided by the DST.

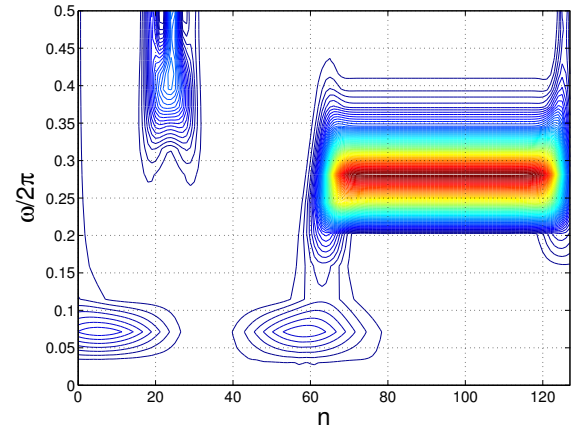


Fig. 8. The spectrogram provided by the WDST.

components. On the other hand, using the WDST with $a = 0.65e^{i0.06\pi}$, one can see that the spectrogram obtained with the WDST is better than DST because the WDST provides an enhanced characterization of harmonic components and, at the same time, offers a better frequency-resolution around $\omega = 0.06$ (rad/sample), as could be see in Fig. 12.

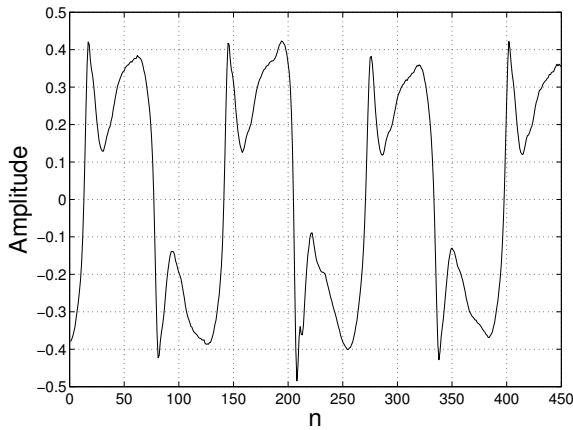


Fig. 9. Non-stationary signal in time domain.

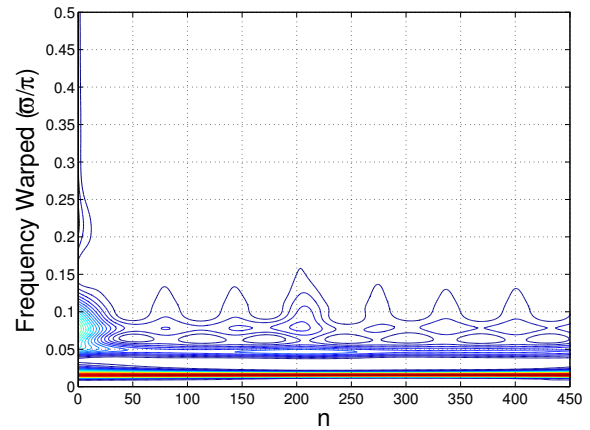


Fig. 12. The spectrogram provided by the W DST.

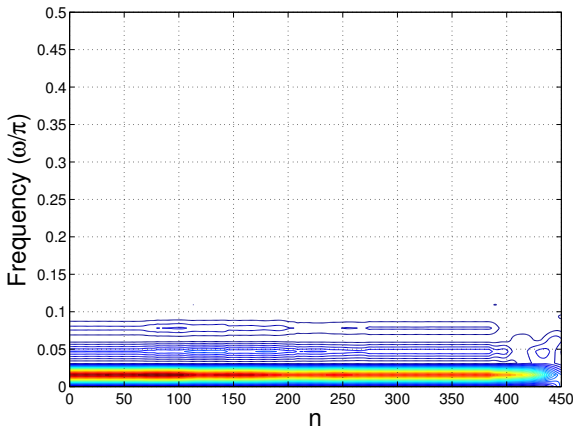


Fig. 10. The spectrogram provided by the ST DFT.

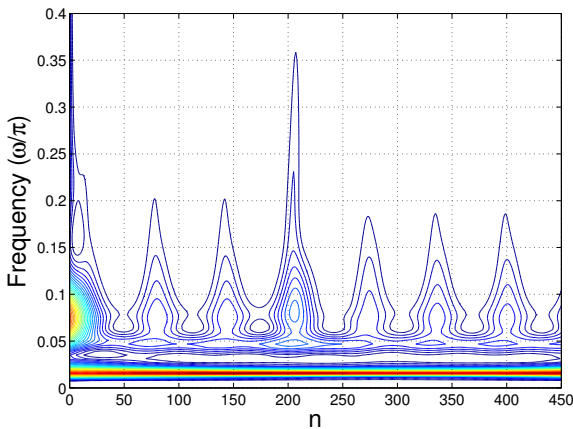


Fig. 11. The spectrogram provided by the DST.

VI. CONCLUSIONS

This contribution introduced the W DST and the W DST for improving the TFR offered by the DST when it is applied to analyze non-stationary signals. Numerical results based on non-stationary signal showed that the W DST is capable of

providing an enhanced spectrogram representation in comparison with the ST DFT and the DST. Due to the widespread use of the DST to analyze electric signals, the replacement of the DST by an another technique that offers an enhanced TFR, such as the that one provided by the W DST, has the potential to improve the performance of several S-transform-based techniques developed so far to analyze non-stationary signals such as electric signals corrupted by transients (e.g., [2][4][5]).

ACKNOWLEDGEMENTS

The authors would like to thanks FINEP, INERGE, CNPq, FAPEMIG, P&D ANEEL, and Smarti9 for their financial support.

REFERENCES

- [1] L. Choen, "Time-frequency distributions - A Review," *Proceedings of the IEEE*, vol. 77, no. 07, pp. 941-981, Jul. 1989.
- [2] I. W. C. Lee and P. K. Dash, "S-Transform-based intelligent system for classification of power quality disturbance signals," *IEEE Trans. on Industrial Electronics*, vol. 50, no. 04, pp. 800-805, Aug. 2003.
- [3] R. G. Stockwell, L. Mansinha, and R. P. Lowe, "Localization of the complex spectrum: The S transform," *IEEE Trans. on Signal Processing*, vol. 44, no. 04, pp. 998-1001, Apr. 1996.
- [4] T. Nguyen and Y. Liao, "Power quality disturbance classification utilizing S-transform and binary feature matrix method," *Signal Processing*, vol. 79, pp. 569-575, 2009.
- [5] M. J. B. Reddy, R. K. Raghupathy, K. P. Venkatesh, and D. K. Mohanta, "Power quality analysis using discrete orthogonal S-transform (DOST)," *Signal Processing*, vol. 23, pp. 661-626, 2013.
- [6] S. Ventosa, C. Simon, M. Schimmel, J. J. Dañobeitia, and A. M ànuel, "The S-transform from wavelet point of view," *IEEE Trans. on Signal Processing*, vol. 56, no. 04, pp. 2771-2780, Jul. 2008.
- [7] A. S. Menezes, "A contribution to spectrum analysis of stationary and non-stationary signals," Ph.D. thesis (in Portuguese), Dept. of Electrical Engineering, Federal University of Juiz de Fora, 2014.
- [8] A. Borowicz, "Warped S-transform for analysing brain waves," *Advanced in Computer Science Research*, vol. 11, pp. 5-16, Jan. 2015.
- [9] A. Makur and S. K. Mitra, "Warped discrete-fourier transform: Theory and applications," *IEEE Trans. on Circuits and Systems*, vol. 48, no. 09, pp. 1086-1093, Sep. 2001.
- [10] S. Franz, S. K. Mitra, and G. Doblinger, "Frequency estimation using warped discrete Fourier transform," *Signal Processing*, vol. 83, pp. 1661-1671, 2006.